

Hot-Fluid Annealing for Crystalline Titanium Dioxide Nanoparticles in Stable Suspension

Jun Lin,[†] Yi Lin,[†] Ping Liu,^{†,‡} Mohammed J. Meziani,[†] Lawrence F. Allard,[§] and Ya-Ping Sun^{*,†}

Contribution from the Department of Chemistry and Center for Advanced Engineering Fibers and Films, Howard L. Hunter Chemistry Laboratory, Clemson University, Clemson, South Carolina 29634-0973, and High Temperature Materials Laboratory, Oak Ridge National Laboratory, Oak Ridge, Tennessee 37831-6062

Received May 2, 2002

Abstract: Titanium dioxide (TiO₂) nanoparticles were synthesized by controlled hydrolysis of titanium alkoxide in reverse micelles in a hydrocarbon solvent. Upon annealing in situ in the presence of the micelles at temperatures considerably lower than those required for the traditional calcination treatment in the solid state, the TiO₂ nanoparticles became highly crystalline but still maintained the same physical parameters and remained in a stable suspension. Thus, the method has allowed the preparation of crystalline TiO₂ nanoparticles that are monodispersed in the same way as they are initially produced in the microemulsion. Effects of the fluid properties on the crystallization of nanoparticles are discussed.

Introduction

Nanoscale semiconductors such as titanium dioxide (TiO₂) have been widely studied for a variety of applications.^{1–3} A commonly applied preparation method for TiO₂ nanoparticles involves the use of microemulsion of reverse micelles in hydrocarbon solvent, which facilitates controlled hydrolysis and condensation of titanium salt in the micellar cavities.⁴ The nanoparticles thus produced are typically amorphous so that a high-temperature calcination process is followed to increase the crystallinity of the nanoparticles.⁵ Crystalline TiO₂ particles are required for many applications, including for example their use as efficient photocatalysts.⁶ In recent years, hydrothermal synthesis has been developed to prepare crystalline TiO₂ nanoparticles without the postcalcination treatment.^{7–9} However, there is the agglomeration of nanoparticles in the hydrothermal synthesis, similar to that found in the crystallization via postcalcination.⁸ Modifications to the hydrothermal synthesis

include the use of surfactant molecules, which prevent the produced nanoparticles from agglomeration in the solid state.⁹ Interestingly, although nanoscale TiO₂ represents one of the most important quantum semiconductor particles, there is hardly a method that allows the preparation of crystalline TiO₂ nanoparticles monodispersed in a stable suspension. The suspended crystalline nanoparticles not only serve as ideal precursors for further materials development but also offer some other unique opportunities, such as enabling studies of their optical, photocatalytic, and other fundamental properties under solution-like conditions.

The formation of crystalline TiO₂ nanoparticles without postcalcination treatment in hydrothermal synthesis demonstrates that solvent may play an important role in the crystallization of nanoscale semiconductors.^{7–9} As a logical extrapolation, especially in light of the recent advances in the processing of nanomaterials by supercritical fluid technology,^{10–15} hot hydrocarbon solvent or fluid may be used to anneal the amorphous

* Corresponding author. E-mail: syaping@clemson.edu.

[†] Clemson University.

[‡] On leave from Fuzhou University, Fuzhou, China.

[§] Oak Ridge National Laboratory.

- (1) (a) Henglein, A. *Chem. Rev.* **1989**, *89*, 1861. (b) Steigerwald, N. L.; Brus, L. E. *Acc. Chem. Res.* **1990**, *23*, 183. (c) Weller, H. *Adv. Mater.* **1993**, *5*, 88. (d) Alivisatos, A. P. *Science* **1996**, *271*, 933. (e) Kamat, P. V.; Meisel, D., Eds., *Semiconductor Nanoclusters-Physical, Chemical, and Catalytic Aspects*; Elsevier: Amsterdam, 1997.
- (2) (a) Schiavello, M., Ed. *Photocatalysis and Environment*; Kluwer Academic Publishers: Dordrecht, The Netherlands, 1988. (b) Ollis, D. F.; Al-Ekabi, H., Eds. *Photocatalytic Purification of Water and Air*; Elsevier: Amsterdam, 1993.
- (3) (a) Fox, M. A.; Dulay, M. T. *Chem. Rev.* **1993**, *93*, 34. (b) Hoffmann, M. R.; Martin, S. T.; Choi, W.; Bahnemann, D. W. *Chem. Rev.* **1995**, *95*, 69. (c) Linsebigler, A. L.; Lu, G.; Yates, J. T. *Chem. Rev.* **1995**, *95*, 735.
- (4) (a) Joselevich, E.; Willner I. *J. Phys. Chem.* **1994**, *98*, 7628. (b) Stathatos, E.; Lianos, P.; Del Monte, F.; Levy, D.; Tsiourvas, D. *Langmuir* **1997**, *13*, 4295. (c) Sant, P. A.; Kamat, P. V. *Phys. Chem. Chem. Phys.* **2002**, *4*, 198.
- (5) (a) Chhabra, V.; Pillai, V.; Mishra, B. K.; Morrone, A.; Shah, D. O. *Langmuir* **1995**, *11*, 3307. (b) Sakai, H.; Kawahara, H.; Shimazaki, M.; Abe, M. *Langmuir* **1998**, *14*, 2208.

- (6) (a) Tanaka, K.; Hisanaga, T.; Riviera, A. P. In *Photocatalytic Purification of Water and Air*; Ollis, D. F., Al-Ekabi, H., Eds.; Elsevier: Amsterdam, 1993; pp 169–178. (b) Augustynski, J. *Electrochim. Acta* **1993**, *38*, 43. (c) Bacsa, R. R.; Kiwi, J. *Appl. Catal. B: Environ.* **1998**, *16*, 19. (d) Yin, H. B.; Wada, Y.; Kitamura, T.; Kambe, S.; Murasawa, S.; Mori, H.; Sakata, T.; Yanagida, S. *J. Mater. Chem.* **2001**, *11*, 1694. (e) Yin, H. B.; Wada, Y.; Kitamura, T.; Sumida, T.; Hasegawa, Y.; Yanagida, S. *J. Mater. Chem.* **2002**, *12*, 378. (f) Hirakawa, T.; Kominami, H.; Ohtani, B.; Nosaka, Y. *J. Phys. Chem. B* **2001**, *105*, 6993. (g) Kim, E. J.; Hahn, S.-H. *Mater. Sci. Eng. A* **2001**, *303*, 24. (h) Ovenstone, J. *J. Mater. Sci.* **2001**, *36*, 1325.
- (7) (a) Moser, J.; Gratzel, M. *J. Am. Ceram. Soc.* **1983**, *105*, 6547. (b) Oguri, Y.; Riman, R. E.; Bowen, H. K. *J. Mater. Sci.* **1988**, *23*, 2897. (c) Bacsa, R. R.; Gratzel, M. *J. Am. Ceram. Soc.* **1996**, *79*, 2185. (d) Yanagisawa, K.; Ovenstone, J. *J. Phys. Chem. B* **1999**, *103*, 7781.
- (8) (a) Wang, C.-C.; Zhang, Z.; Ying, J. Y. *Nanostruct. Mater.* **1997**, *9*, 583. (b) Kim, S. J.; Park, S. D.; Jeong, Y. H.; Park, S. *J. Am. Ceram. Soc.* **1999**, *82*, 927. (c) Yang, Y.; Mei, S.; Ferreira, J. M. F. *J. Am. Ceram. Soc.* **2000**, *83*, 1361.
- (9) (a) Zhang, Z.; Wang, C.-C.; Zakaria, R.; Ying, J. Y. *J. Phys. Chem. B* **1998**, *102*, 10871. (b) Wang, C.-C.; Ying, J. Y.; *Chem. Mater.* **1999**, *11*, 3113. (c) Wu, M. M.; Long, J. B.; Huang, A. H.; Luo, Y. J.; Feng, S. H.; Xu, R. R. *Langmuir* **1999**, *15*, 8822.

semiconductor nanoparticles synthesized and encapsulated in micellar cavities under the conditions that cause no significant damages to the micellar structures and the stable suspension. In this paper, we report the synthesis of TiO₂ nanoparticles in reverse micelles in cyclohexane and the crystallization of these nanoparticles via annealing in situ in the presence of the micelles at temperatures considerably lower than those required for the traditional calcination treatment in the solid state. Except for their high crystallinity, the annealed TiO₂ nanoparticles maintain the same physical parameters and remain individually dispersed to form a stable suspension in the microemulsion. Results from the characterization of the crystalline TiO₂ nanoparticles using techniques such as X-ray powder diffraction and high-resolution electron microscopy are presented. The potential for the further development of the hot-fluid annealing process into a generalized method for stable suspension of agglomeration-free crystalline nanoparticles is discussed.

Experimental Section

Materials. Sodium bis(2-ethylhexyl) sulfosuccinate (AOT, 99%) was purchased from Sigma. Titanium isopropoxide (97%) was obtained from Alfa Aesar. All organic solvents were spectrophotometry grade and used as received. Water was deionized and purified by being passed through a Labconco Water purification system.

Nanoparticle Preparation. In a typical experiment, water (0.9 mL) and the surfactant AOT (5 g) were added to cyclohexane (50 mL), and the mixture was stirred to form an apparently homogeneous microemulsion (W_0 , defined as the molar ratio of water to surfactant, of 4.5). For the preparation of TiO₂ nanoparticles, a solution of titanium isopropoxide (3 mL) in 1-hexanol (30 mL) was added to the microemulsion, followed by slow stirring to allow hydrolysis of the titanium salt in the reverse micellar cavities. The nanoparticles thus formed were protected by the micellar structures, forming a solution-like homogeneous suspension.

AOT-protected water-in-cyclohexane microemulsions of other W_0 values (9, 15, and 18) were similarly prepared by varying the amount of AOT while keeping the amount of water constant. The reverse micellar cavities in these microemulsions were also used for the hydrolysis of titanium isopropoxide to form TiO₂ nanoparticles of different average sizes.

Annealing. In a typical experiment, a microemulsion of micelles-protected TiO₂ nanoparticles in cyclohexane (9 mL) was deoxygenated in a test tube via purging with dry nitrogen gas for ~10 min. The test tube was then placed in a stainless steel reactor (High Pressure Equipment Co.). After further purging with nitrogen gas, the reactor was sealed and heated to 250 °C in a furnace. Since the reactor was not completely filled, the system pressure was close to the vapor pressure of cyclohexane (390 psia at 250 °C). After annealing at the constant temperature for 7 h, the reactor was quickly cooled to the ambient temperature to allow the retrieval of the suspended TiO₂ nanoparticles in the test tube for characterization.

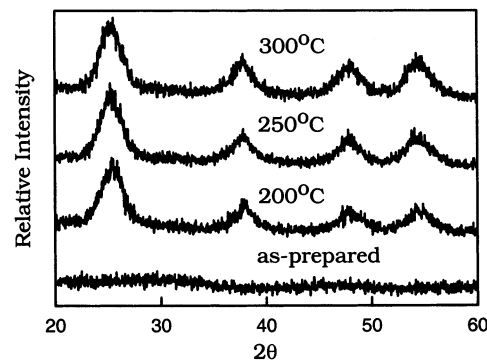


Figure 1. X-ray powder diffraction patterns of the TiO₂ nanoparticle samples as-prepared in the microemulsion ($W_0 = 4.5$) and after annealing in near-critical and supercritical cyclohexane.

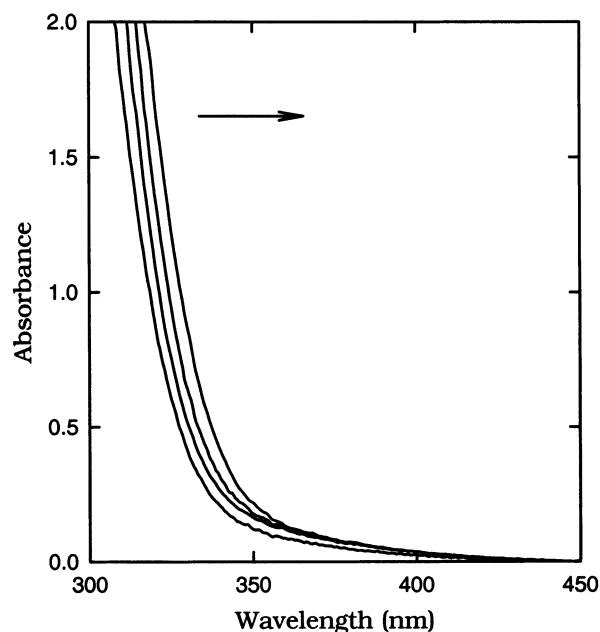


Figure 2. UV/vis absorption spectra of the TiO₂ nanoparticles obtained in microemulsions with W_0 of (in the direction of arrow) 4.5, 9, 15, and 18.

Measurements. UV/vis absorption spectra were recorded on a Shimadzu UV-2101PC spectrophotometer. X-ray powder diffraction measurements were performed on a Scintag XDS-2000 system. Transmission electron microscopy (TEM) images were obtained using Hitachi 7000 and Hitachi HF-2000 TEM instruments.

Results and Discussion

The TiO₂ nanoparticles prepared in the microemulsion at room temperature are amorphous according to X-ray powder diffraction analysis (Figure 1), in agreement with what have been reported in the literature.⁵ The UV/vis absorption spectra of the nanoparticles are shown in Figure 2. The absorption onsets are at 330–350 nm, consistent with the prediction in terms of the Brus equation.¹⁶

For the crystallization of the TiO₂ nanoparticles in the suspension under agglomeration-free condition, the amorphous nanoparticles were thermally treated in the presence of the AOT-stabilized reverse micelles in cyclohexane at a constant temperature (as high as 300 °C) for up to 48 h. The thermally annealed TiO₂ nanoparticles remained well-suspended without precipitation. The effect of the thermal treatment on the

- (10) Sun, Y.-P.; Rollins, H. W.; Jayasundera, B.; Meziani, M. J.; Bunker, C. E. In *Supercritical Fluid Technology in Materials Science and Engineering: Synthesis, Properties, and Applications*; Sun, Y.-P., Ed.; Marcel Dekker: New York, 2002; p 491.
- (11) (a) Watkins, J. J.; McCarthy, T. J. *Chem. Mater.* **1995**, *7*, 1991. (b) Blackburn, J. M.; Long, D. P.; Cabanas, A.; Watkins, J. J. *Science* **2001**, *294*, 141.
- (12) (a) Ji, M.; Chen, X. Y.; Wai, C. M.; Fulton, J. L. *J. Am. Chem. Soc.* **1999**, *121*, 2631. (b) Ohde, H.; Rodriguez, J. M.; Ye, X. R.; Wai, C. M. *Chem. Commun.* **2000**, *23*, 2353.
- (13) (a) Holmes, J. D.; Bhargava, P. A.; Korgel, B. A.; Johnston, K. P. *Langmuir* **1999**, *15*, 6613. (b) Shah, P. C.; Holmes, J. D.; Doty, R. C.; Johnston, K. P.; Korgel, B. A. *J. Am. Chem. Soc.* **2000**, *122*, 4245.
- (14) Cason, J. P.; Roberts, C. B. *J. Phys. Chem. B* **2000**, *104*, 1217.
- (15) (a) Sun, Y.-P.; Rollins, H. W.; Guduru, R. *Chem. Mater.* **1999**, *11*, 7. (b) Sun, Y.-P.; Guduru, R.; Lin, F.; Whiteside, T. *Ind. Eng. Chem. Res.* **2000**, *39*, 4663. (c) Sun, Y.-P.; Atorngitjawan, P.; Meziani, M. J. *Langmuir* **2001**, *17*, 5707.

(16) Brus, L. E. *J. Chem. Phys.* **1983**, *79*, 5566.

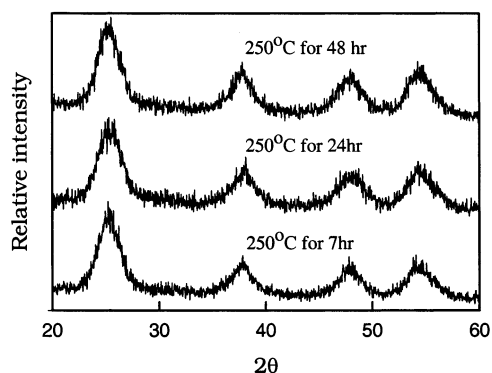


Figure 3. Effects of the annealing time on the crystallization of TiO₂ nanoparticles.

Table 1. Effects of Experimental Conditions on Observed TiO₂ Nanoparticle Sizes

W_0	annealing temp ^a (°C)	annealing time (h)	av particle size ^b (nm)
4.5	200	7	3.9
4.5	250	7	4.1
4.5	250	24	4.3
4.5	250	48	4.3
4.5	300	7	4.3
9	250	24	4.9
15	250	24	5.4
18	250	24	5.7

^a The system pressure was approximately the vapor pressure of cyclohexane (195, 390, and 780 psia at 200, 250, and 300 °C, respectively).

^b Estimated from the broadening in X-ray powder diffraction peaks (eq 1).

crystallinity of the TiO₂ nanoparticles was evaluated via X-ray powder diffraction analysis. As shown in Figure 1, the annealing temperature had significant effect on the crystallinity of the resulting TiO₂ nanoparticles, with high crystallinity for annealing at 250 and 300 °C and with the diffraction patterns corresponding to pure anatase TiO₂. The broadening in the diffraction peak (corresponding to the 101 plane in the crystal structure) was used to estimate the average TiO₂ nanocrystal size in terms of the Debye–Scherer equation.¹⁷

$$D = K\lambda/(\beta \cos \theta) \quad (1)$$

where D is the average nanocrystal diameter in angstrom, β is the corrected band broadening (full width at half-maximum (fwhm)), K is a constant related the crystallite shape and the way in which D and β are defined, λ is the X-ray wavelength, and θ is the diffraction angle. The average diameter thus estimated for the TiO₂ nanoparticles prepared in the microemulsion of $W_0 = 4.5$ and annealed at 250 °C for 24 h is 4.3 nm.

For the annealing at 250 °C the results are insensitive to the heating time. Compared in Figure 3 are X-ray powder diffraction patterns of the TiO₂ nanoparticles annealed for 7, 24, and 48 h under otherwise the same experimental conditions. The average particle sizes estimated from the diffraction peak broadening are rather similar for these nanoparticles annealed for varying periods of time (Table 1).

The crystalline TiO₂ nanoparticles from the thermal annealing in cyclohexane were also analyzed by TEM. For the analysis, a small drop of the suspension was used to deposit the nanoparticles on a copper grid. Shown in Figure 4 are typical high-resolution TEM images of the TiO₂ nanoparticles. The

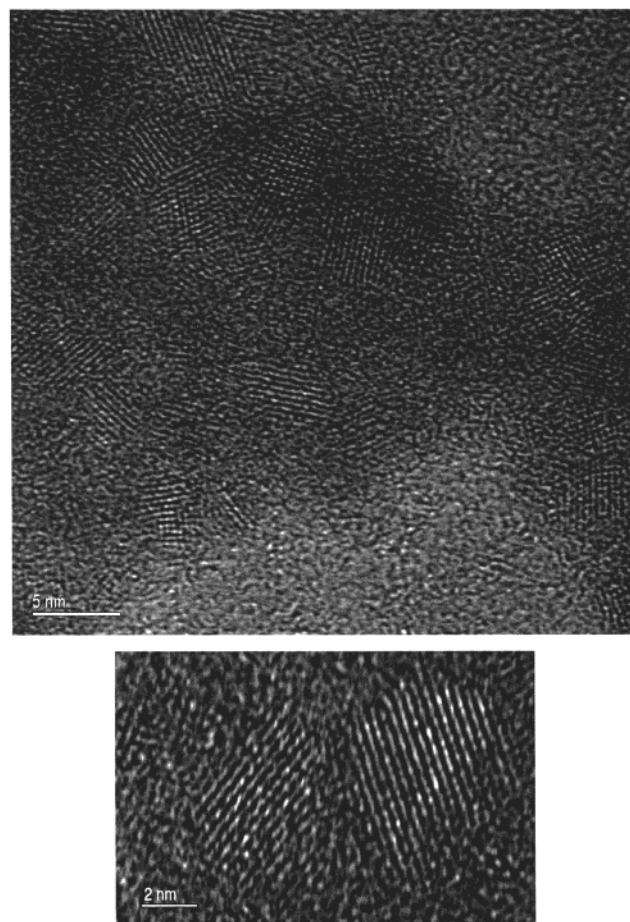


Figure 4. High-resolution TEM images of the crystalline TiO₂ nanoparticles.

thermally annealed nanoparticles are obviously crystalline, with clearly visible lattice fringes corresponding to anatase TiO₂. For the nanoparticles prepared in the microemulsion with W_0 of 4.5 and annealed at 250 °C for 24 h, a statistical analysis of 190 particles in TEM images yielded an average particle diameter of 4.4 nm and a size distribution standard deviation of 0.5 nm. The average TiO₂ particle diameter thus obtained from the TEM analysis is almost the same as the value estimated from the broadening in the X-ray powder diffraction peak. Such an excellent agreement may be considered evidence for the fact that the crystal grain size and particle size of the annealed TiO₂ nanoparticles are essentially the same.

The average size of TiO₂ nanoparticles is dependent on the micellar cavity size, which is dictated by the W_0 value.¹⁸ A larger W_0 value corresponds to reverse micelles of larger cavities, resulting in the formation of larger TiO₂ nanoparticles. In this study, AOT-stabilized water-in-cyclohexane microemulsions with W_0 values of 9, 15, and 18 were also used to prepare TiO₂ nanoparticles. These nanoparticles were annealed in situ in the microemulsions at 250 °C for 24 h. Except for their high crystallinity, the annealed TiO₂ nanoparticles exhibited no other obvious changes, remaining well-suspended in the microemulsions. The X-ray powder diffraction patterns of the crystalline TiO₂ nanoparticles corresponding to the microemulsions of

(17) Klug, H. P.; Alexander, L. E. *X-ray Diffraction Procedures*; John Wiley & Sons: New York, 1959.

(18) (a) Pileni, M. P. *J. Phys. Chem.* **1993**, *97*, 6961. (b) Liseiecki, I.; Pileni, M. P. *J. Am. Chem. Soc.* **1993**, *97*, 6961. (c) Eastoe, J.; Hetherington, K. J.; Sharpe, D.; Dong, J.; Heenan, R. K.; Steyler, D. *Langmuir* **1996**, *12*, 3876. (d) Pileni, M. P. *Cryst. Res. Technol.* **1998**, *33*, 1155.

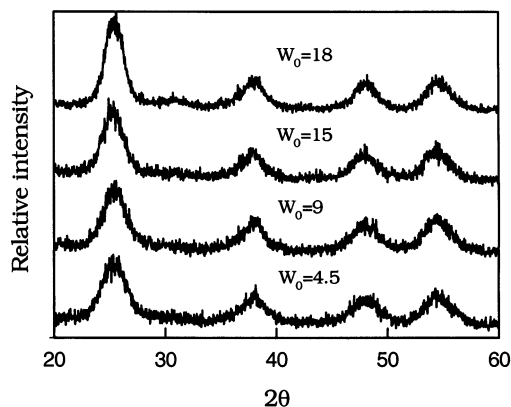


Figure 5. X-ray powder diffraction patterns of the TiO₂ nanoparticles prepared and annealed in different microemulsions.

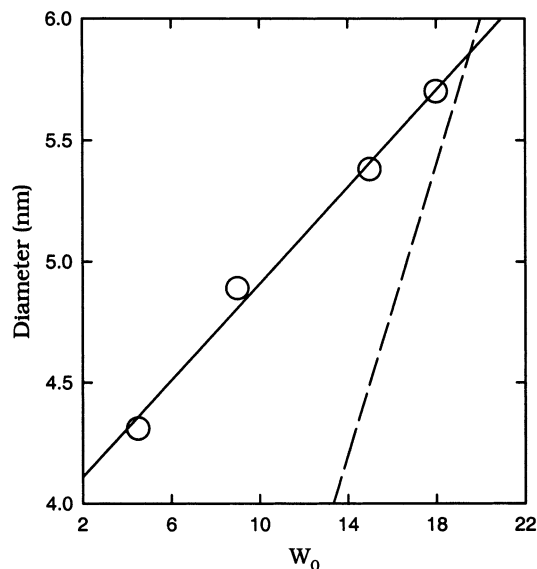


Figure 6. Relationship between the average size of the TiO₂ nanoparticles and the W_0 value is close to linear (O, —), but it is different from the proportional dependence of the micellar cavity size on the W_0 value (—).

different W_0 values are shown in Figure 5. The average particle sizes were estimated from the peak broadening in terms of eq 1. The results show that larger crystalline TiO₂ nanoparticles are indeed obtained with the microemulsions of larger W_0 values. As illustrated in Figure 6, the average size of crystalline TiO₂ nanoparticles is close to linearly dependent on the W_0 value of the microemulsion in which the nanoparticles are produced and annealed.

For the dependence of micellar cavity size on the W_0 value, a linear relationship widely cited in the literature is as follows.^{19,20}

$$d = \alpha W_0 \quad (2)$$

where d is the micellar cavity diameter in angstrom. The proportionality constant α is typically 3, as supported by the

results from neutron scattering experiments.²⁰ However, eq 2 is known to be valid only for large W_0 values. Significant deviations from experimental results (underestimating the micelle sizes) for small W_0 values (<10) have been reported in the literature.¹⁹ The comparison in Figure 6 shows that the W_0 dependence of the TiO₂ nanoparticle size follows a different linear relationship from eq 2, with the two lines crossing at W_0 of ~ 19 . This is consistent with what is known in the literature, namely, that the actual nanoparticle sizes are larger than those predicted by eq 2, and the difference is more pronounced at smaller W_0 values. Nevertheless, the empirical linear $D - W_0$ relationship shown in Figure 6 is useful in the control of the average nanoparticle size via adjusting the W_0 value of the microemulsion.

In the hot-fluid annealing, temperature is obviously important, but the solvent also plays a critical role. Without the solvent, the annealing of the micelles-protected TiO₂ nanoparticles in solid state at the same temperatures resulted in essentially no crystallization. The mechanism for the crystallization in hot-fluid annealing is unclear and likely complex. It may involve collisions of the elements on nanoparticles with solvent molecules, which coupled with a moderately high temperature probably cause localized melting and lattice rearrangement. The use of cyclohexane, a solvent with a moderate critical temperature (279.6 °C), as the annealing fluid was to take advantage of the unique properties of a supercritical fluid.²¹ The low density and associated low viscosity (high diffusivity) and low surface tension of supercritical fluids have found them widespread applications in extraction and chromatography.^{22,23} The same properties may in principle benefit the crystallization process by allowing more efficient and complete access of the nanoparticle surface (including those small cavities and defects) by the supercritical solvent molecules. However, as in extraction and chromatography, supercritical fluid is not a requirement in the in situ annealing of amorphous nanoparticles. Similar thermal treatment at 250 °C in solvents of higher critical temperatures, such as tetradecane (critical temperature 420 °C), also resulted in the crystallization of TiO₂ nanoparticles, though the X-ray diffraction results appeared weaker and broader. A direct comparison of annealing results with different solvents has been complicated by the variation in solvent parameters other than the critical temperature and some technical difficulties. Further investigations are required.

A practically more important feature of the hot-fluid annealing process is that the crystallization of nanoparticles is accomplished in situ in the reverse micelles. The resulting crystalline nanoparticles remain monodispersed in stable suspension without any significant agglomeration effects. The process may be generalized to offer a convenient method for the preparation of micelles-protected nanocrystalline particles from a variety of materials.

Acknowledgment. Financial support from the Department of Energy (Grant DE-FG02-00ER45859) and the Center for Advanced Engineering Fibers and Films (NSF-ERC at Clemson

- (19) (a) Zulauf, M.; Eicke, H. F. *J. Phys. Chem.* **1979**, *83*, 480. (b) Kotlarchyk, M.; Chen, S.-H.; Huang, J. S.; Kim, M. W. *Phys. Rev. A* **1984**, *29*, 2054. (c) Pileni, M. P.; Zemb, T.; Petit, C. *Chem. Phys. Lett.* **1985**, *118*, 414. (d) Brochette, P.; Petit, C.; Pileni, M. P. *J. Phys. Chem.* **1988**, *92*, 3505.
- (20) Robinson, B. H.; Topraciaglu, C.; Dore, J.; Chieux, P. *J. Chem. Soc., Faraday Trans. 1* **1984**, *80*, 13.

- (21) The properties of a subcritical fluid at a temperature close to the critical temperature are similar to those of supercritical fluids.
- (22) McHugh, M. A.; Krukonis, V. J. *Supercritical Fluid Extraction—Principles and Practice*; Butterworth: Boston, MA, 1993.
- (23) Bunker, C. E.; Rollins, H. W.; Sun, Y.-P. In *Supercritical Fluid Technology in Materials Science and Engineering: Synthesis, Properties, and Applications*; Sun, Y.-P., Ed.; Marcel Dekker: New York, 2002; p 1, and references therein.

University) is gratefully acknowledged. We also acknowledge the sponsorship by the Assistant Secretary for Energy Efficiency and Renewable Energy, Office of Transportation Technologies, as part of the High Temperature Materials Laboratory User

Program, Oak Ridge National Laboratory, managed by UT-Battelle, LLC, for the Department of Energy (Grant DE-AC05-00OR22725).

JA0206341